Institut für Numerische Simulation
Rheinische Friedrich-Wilhelms-Universität Bonn

Wegelerstraße 6 • 53115 Bonn • Germany
phone +49 228 73-3427 • fax +49 228 73-7527
www.ins.uni-bonn.de

J. Adelsberger, P. Esser, M. Griebel,
S. Groß, M. Klitz, A. Rüttgers

3D incompressible two-phase flow benchmark computations for rising droplets

INS Preprint No. 1401

March 2014

11th World Congress on Computational Mechanics (WCCM XI)
5th European Conference on Computational Mechanics (ECCM V)
6th European Conference on Computational Fluid Dynamics (ECFD VI)
E. Oñate, J. Oliver and A. Huerta (Eds)

3D INCOMPRESSIBLE TWO-PHASE FLOW BENCHMARK COMPUTATIONS FOR RISING DROPLETS

Jutta Adelsberger*, Patrick Esser†, Michael Griebel*, Sven Groß†, Margrit Klitz* and Alexander Rüttgers*

* Institute for Numerical Simulation (INS), University of Bonn
Wegelerstr. 6, D-53115 Bonn, Germany
e-mail: {adelsberger,griebel,klitz,ruettgers}@ins.uni-bonn.de,
web page: www.ins.uni-bonn.de

†Chair for Numerical Mathematics (IGPM), RWTH Aachen University
Templergraben 55, D-52056 Aachen, Germany
e-mail: {pesser,gross}@igpm.rwth-aachen.de,
web page: www.igpm.rwth-aachen.de

Key words: Two-phase Flow, Benchmark Simulations, Three-dimensional Computations, Parallel Computing, Rising Droplets

Abstract. We perform 3D incompressible two-phase flow simulations of rising droplets. Based on a similar 2D benchmark, a 3D benchmark configuration with two test cases is formulated in which we compare the flow solvers DROPS, NaSt3DGPF and OpenFOAM. All codes adopt different numerical techniques. We define several quantities of interest and investigate their temporal evolution in both test cases. For most benchmark variables we obtain a high level of agreement and establish reference data for other flow solvers.

1 INTRODUCTION

The modeling and simulation of three-dimensional two-phase flows is still an area of active research. Various approaches have been developed to improve conservation of mass, capturing of the fluid's interface or computation of interfacial surface tension. For the validation of these new methods, qualitative benchmark data is required.

We perform 3D incompressible two-phase flow simulations of rising droplets. Based on a similar 2D benchmark proposed in [1], a 3D benchmark configuration with two test cases is formulated in which we compare the flow solvers DROPS [2], NaSt3DGPF [3] and OpenFOAM [4]. All codes adopt different numerical techniques. We list the main features of each code in Table 1.

	DROPS	NaSt3D	OpenFOAM
developer	IGPM, RWTH Aachen	INS, University of Bonn	open source
space discretization	XFEM	finite differences	finite volumes
interface capturing	level set	level set	VOF
time discretization	implicit θ-scheme	Adams-Bashforth 2nd	implicit Euler

Table 1: Comparison of the code features and schemes used for the 3D benchmark.

2 MATHEMATICAL FLOW MODEL

Let $\Omega \subset \mathbb{R}^3$ be a polyhedral domain containing two different immiscible incompressible phases $\Omega_1(t), \Omega_2(t)$ with $\bar{\Omega} = \bar{\Omega}_1 \cup \bar{\Omega}_2$ and $\Omega_1 \cap \Omega_2 = \emptyset$. The interface separating both phases is denoted by $\Gamma(t) = \partial\Omega_1(t) \cap \partial\Omega_2(t)$. The standard model for incompressible two-phase flow consists of the Navier-Stokes equations for pressure $p = p(\mathbf{x}, t)$ and velocity $\mathbf{u} = \mathbf{u}(\mathbf{x}, t)$ in the subdomains Ω_i, $i = 1, 2$, with the coupling conditions

$$[\boldsymbol{\sigma}\mathbf{n}]_\Gamma = \tau\kappa\mathbf{n}, \qquad [\mathbf{u}]_\Gamma = 0$$

at the interface Γ, i. e., we assume that surface tension balances the jump of normal stresses and that $\mathbf{u}$ is continuous across the interface. Here, τ and κ denote the surface tension coefficient and interfacial curvature, respectively, and $\mathbf{n}$ is the unit normal on Γ pointing from Ω_2 into Ω_1. Furthermore, $\boldsymbol{\sigma} = -p\mathbf{I} + \mu\mathbf{D}(\mathbf{u})$ denotes the stress tensor with $\mathbf{D}(\mathbf{u}) = \nabla\mathbf{u} + \nabla\mathbf{u}^\mathsf{T}$ the deformation tensor and μ the dynamic viscosity. Combined with the conservation laws for mass and momentum, we obtain the following standard model

$$\rho_i \left(\frac{\partial}{\partial t} + \mathbf{u} \cdot \nabla \right) \mathbf{u} - \operatorname{div} \boldsymbol{\sigma} = \rho_i \mathbf{g} \qquad \text{in } \Omega_i \times [0, T], \quad i = 1, 2, \tag{1}$$

$$\operatorname{div} \mathbf{u} = 0 \qquad \text{in } \Omega_i \times [0, T], \quad i = 1, 2, \tag{2}$$

$$[\boldsymbol{\sigma}\mathbf{n}]_\Gamma = \tau\kappa\mathbf{n}, \qquad [\mathbf{u}]_\Gamma = 0 \qquad \text{at } \Gamma \times [0, T], \tag{3}$$

cf. for example [2]. The densities ρ_i, dynamic viscosities μ_i, $i = 1, 2$, and the gravitational force $\mathbf{g}$ are assumed to be constant.

In general, the location of the interface $\Gamma(t)$ is unknown. Only the position of the initial interface $\Gamma(0)$ is assumed to be given, which is then advected by the local velocity field $\mathbf{u}$. There are different approaches in the literature, where most of them can be classified as either interface-tracking or interface-capturing techniques. The codes applied in this benchmark use interface-capturing strategies, either the level set or VOF method, cf. Table 1. To this end, equations (1)–(3) are augmented by an additional evolution equation for the respective indicator function, e.g., $\frac{\partial\varphi}{\partial t} + \mathbf{u} \cdot \nabla\varphi = 0$ in $\Omega \times [0, T]$ for the level set function φ.

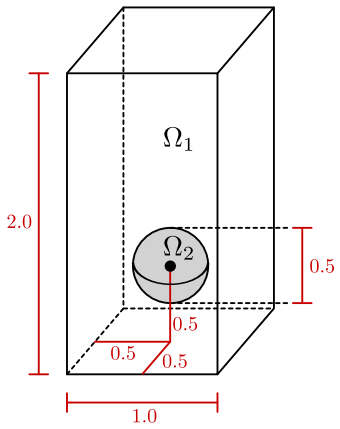

Figure 1: Initial configuration in both test cases.

	test case 1	test case 2
ρ_1	1000	1000
μ_1	10	10
ρ_2	100	1
μ_2	1	0.1
τ	24.5	1.96

Table 2: Material properties for test case 1 and 2.

3 DEFINITION OF THE BENCHMARK

Consider a cuboid tank $\Omega = [0,1] \times [0,2] \times [0,1]$ and a droplet $\Omega_2 = \Omega_2(t) \subset \Omega$ which is lighter than the surrounding fluid $\Omega_1 = \Omega \setminus \Omega_2$ (cf. Figure 1). The final time T is prescribed as $T = 3$ and $T = 3.5$ for the test cases 1 and 2, respectively. We assume no-slip boundary conditions, i. e., $\mathbf{u} = 0$ on $\partial\Omega$. The initial condition for the Navier-Stokes equations is given by $\mathbf{u}(0) = 0$. The initial droplet is assumed to be spherical with radius $r = 0.25$ and center point $\mathbf{x}_c = (0.5, 0.5, 0.5)^\mathsf{T}$, i. e., fluid phase 2 is initially given by

$$\Omega_2(0) = \{\mathbf{x} \in \Omega \,|\, \|\mathbf{x} - \mathbf{x}_c\| \leq r\}.$$

Due to buoyancy effects, the droplet will start to rise and change its shape.

The two test cases are defined according to the material properties given in Table 2 and with a gravitational force $\mathbf{g} = (0, -0.98, 0)^\mathsf{T}$. These parameters are taken from the 2D two-phase flow benchmark proposed in [1]. For test case 1, the density and viscosity ratio $\rho_1/\rho_2 = \mu_1/\mu_2 = 10$ is rather moderate, whereas for the second test case, we have larger ratios $\rho_1/\rho_2 = 1000$ and $\mu_1/\mu_2 = 100$ which are roughly the same as for an air bubble in water. For test case 1, the droplet becomes ellipsoidal-shaped. In test case 2, a break-up of the droplet is possible due to the lower surface tension. According to the classification by Clift et al. [5], test case 1 can be assigned to the ellipsoidal regime and test case 2 lies somewhere between the skirted and dimpled ellipsoidal-cap regimes.

3.1 Quantities of interest

In the following, we define four time-dependent quantities of interest which are used to compare the different simulations with each other. The first one is the *barycenter* $\bar{\mathbf{x}}$ of the droplet,

$$\bar{\mathbf{x}}(t) = |\Omega_2|^{-1} \int_{\Omega_2(t)} \mathbf{x}\, d\mathbf{x},$$

with $|\Omega_2| := \text{meas}_3\,\Omega_2 = \int_{\Omega_2} 1\,d\mathbf{x}$ the volume of the droplet. Second, its *rise velocity* $\bar{\mathbf{u}}$ is given by

$$\bar{\mathbf{u}}(t) = |\Omega_2|^{-1} \int_{\Omega_2(t)} \mathbf{u}\,d\mathbf{x}.$$

The *diameter* $\mathbf{d}(t) = (d_1(t), d_2(t), d_3(t))^\mathsf{T}$ denotes the droplet's maximum extension in each coordinate direction, i.e.,

$$d_i(t) = \max_{\mathbf{x},\mathbf{y}\in\Omega_2(t)} |x_i - y_i|, \qquad i = 1, 2, 3.$$

The last quantity of interest measures how much the droplet's shape differs from a sphere. The *sphericity* Ψ is defined in [6] as follows,

$$\Psi(t) = |\Gamma(t)|^{-1}\,\pi^{1/3}(6|\Omega_2|)^{2/3},$$

which is the surface area of a sphere with volume $|\Omega_2|$ divided by the surface area $|\Gamma(t)| := \text{meas}_2\,\Gamma(t) = \int_{\Gamma(t)} 1\,ds$ of the droplet. Ψ is equal to 1 if Ω_2 is a sphere and decreases the more the droplet is flattened.

4 NUMERICAL RESULTS

4.1 Simulation parameters

For the **DROPS** simulations, the tetrahedral grid is adaptively refined near the interface, following the position of the droplet. A regular initial grid with $4 \times 8 \times 4$ subcubes each subdivided into 6 tetrahedra is used, which is then 3 times adaptively refined near the interface, leading to a mesh size of $h = \frac{1}{32}$ within the refinement zone. Finite elements are used for spatial discretization, employing P_2-FEM for the velocity, P_1-XFEM for the pressure and P_2-FEM for the level set. For temporal discretization, the implicit θ-scheme with $\theta = 0.5$ and time step size $\Delta t = 2.5 \cdot 10^{-4}$ is applied. The linearized systems are solved by a preconditioned GCR method using V-cycle multigrid as velocity preconditioner and a Cahouet-Chabard Schur complement preconditioner for the pressure field. Re-initialization of the level set function φ is performed with a fast marching method whenever $\|\nabla\varphi\|_2 \notin [\frac{1}{10}, 10]$ near the interface. The droplet's mass conservation is enforced by a simple global volume correction described in [2]. Each of the simulations required about two weeks computing time on a single processor.

In both test cases, **NaSt3DGPF** uses an equidistant finite difference grid with $121 \times 241 \times 121$ grid cells. For temporal discretization, Chorin's projection method is employed to decouple the fluid velocities and the pressure field. The velocities are treated explicitly with a 2nd-order Adams-Bashforth scheme. The pressure field is computed by solving a Poisson-type equation in each time step. For the solution of the pressure Poisson problem, NaSt3DGPF uses an AMG-preconditioned BiCGStab solver. The convective terms in the momentum equations are treated with a 2nd-order SMART scheme which showed reduced numerical diffusion in previous studies compared to an also implemented

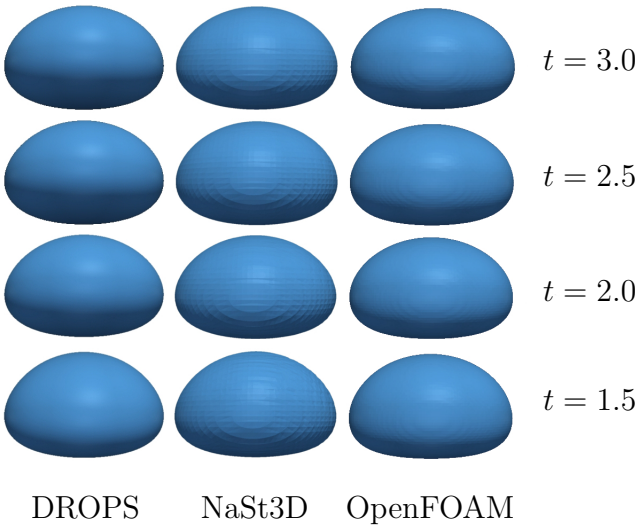

Figure 2: Droplet rise in test case 1.

5th-order WENO scheme. During the simulation, the droplet's mass was conserved with a local volume correction method according to [7]. All simulations with NaSt3DGPF were performed on 32 processors of the HPC cluster *Siebengebirge* featuring 160 Intel Xeon X7560 2.226 GHz CPU cores and a main memory of 2560 GB in total. The system has a Linpack performance of 1349 GFlops/s with a parallel efficiency of 93%. Both parallel simulations required about one week of computing time. A typical time step width of the adaptive temporal scheme lies in the order of $\mathcal{O}(10^{-4})$.

In **OpenFOAM**, we use an equidistant grid with $128 \times 256 \times 128$ cuboid cells and employ the interFoam solver version 2.2.2 for two incompressible fluids capturing the interface with a VOF method [4]. Finite volumes are used as spatial discretization and the implicit Euler method as temporal discretization with time step size $\Delta t = 10^{-4}$. For the convective terms in the momentum and phase equations, we use a limited linear and a van Leer scheme, respectively, and a specialized interface compression scheme to gain smoother interfaces. As pressure and phase corrector, a merged PISO/SIMPLE algorithm is implemented with three correction steps for pressure and two sub-cycles for the correction of the interface. The solvers are a preconditioned BiCG with diagonal incomplete-LU preconditioner for the velocity and a Cholesky-preconditioned CG for the pressure. Both test cases were performed on 32 processors of the HPC cluster *Siebengebirge* and required about 2.5 days of computing time each.

4.2 Test case 1

Figure 2 illustrates the droplet's evolution in test case 1 over time. As illustrated, the spherical droplet is extended in directions x and z perpendicular to the flow and compressed in the flow direction y. At $t \approx 2.0$, the droplet reaches a stable ellipsoidal shape up to the final state of the simulation.

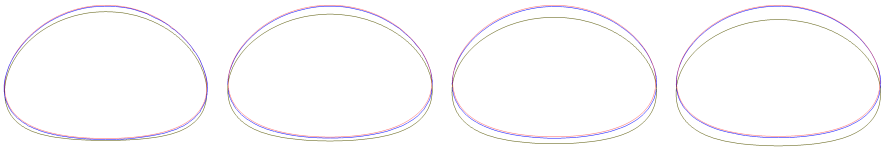

Figure 3: Contour comparison of DROPS (blue), NaSt3D (red), OpenFOAM (olive) for test case 1.

For a better comparison of the actual droplet shape, Figure 3 plots the two-dimensional contour on the x/y-plane with normal $\mathbf{n} = (0, 0, 1)^\mathsf{T}$ through the droplet's center. The contour lines of DROPS (blue) and NaSt3DGPF (red) closely resemble each other. The contour line of OpenFOAM (olive), although similar in its shape, is shifted in the vertical direction y compared to the other two flow solvers.

Figure 4 shows the y-component of the droplet's barycenter position $\bar{\mathbf{x}}$ over time. In the early state of the simulation up to $t \approx 1$, the position $\bar{\mathbf{x}}$ is nearly identical in all simulations. The vertical position of the droplet in OpenFOAM is lower than for DROPS and NaSt3DGPF as indicated in the contour plots in Figure 3. The final state of the simulation is visualized in a zoomed extract on the RHS of Figure 4. The position of this extract is indicated with a black rectangle on the LHS of Figure 4. Note that all subsequent plots of quantities of interest also have a zoomed part on the RHS of the corresponding figure.

The droplet's rise velocity is visualized in Figure 5. In the early state of the simulation, the velocity component v of $\bar{\mathbf{u}}$ increases from its initial value zero up to a maximum value in the order of 0.35–0.36 at about $t \approx 0.9$. The maximum velocity is roughly 0.357 in DROPS, 0.358 in NaSt3DGPF and 0.352 in OpenFOAM. The rise velocity in DROPS then decreases to $v \approx 0.347$, to $v \approx 0.35$ in NaSt3DGPF and to $v \approx 0.33$ in OpenFOAM. Due to the differences in the rise velocity in the final part of the simulation, the droplet positions are shifted in Figure 3 and Figure 4.

In the following, we concentrate on an analysis of the droplet's shape. For this purpose, Figure 6 shows the different components of the droplet's diameter $\mathbf{d}$ over time. During the simulation, d_1 and d_3 increase up to a final value of about 0.58 in all three simulations. On the other hand, the extension d_2 in y-direction is 0.37 for DROPS and NaSt3DGPF and about 0.355 for OpenFOAM as indicated on the RHS of Figure 6. These results suggest that the droplet in the DROPS and NaSt3DGPF simulations has a slightly more spherical shape than in the case of OpenFOAM.

A measure of the droplet's similarity with its initial spherical form is given by the sphericity Ψ. Figure 7 displays Ψ over time. Due to the droplet's compression in vertical direction, the sphericity decreases from 1 to about 0.96 for DROPS and NaSt3DGPF and to $\Psi \approx 0.955$ for OpenFOAM (cf. RHS of Figure 7). The slightly lower sphericity in OpenFOAM primarily results from a stronger compression in vertical direction as indicated in Figure 6. DROPS and NaSt3DGPF predict similar sphericity values at the end of the simulation but with non-smooth jumps in the case of DROPS. This results

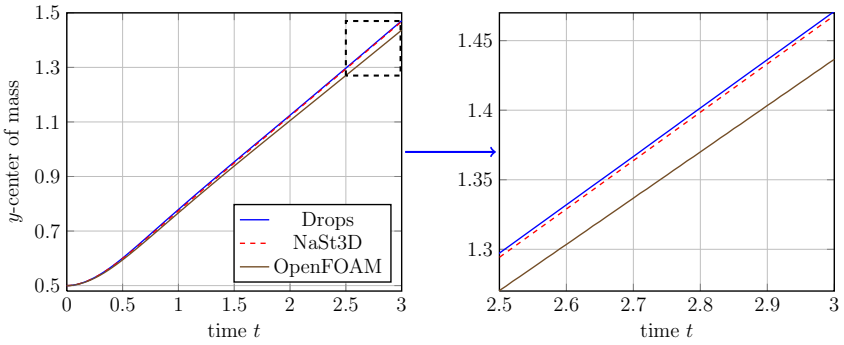

Figure 4: Center of mass $\bar{\mathbf{x}}$ in y-direction for test case 1.

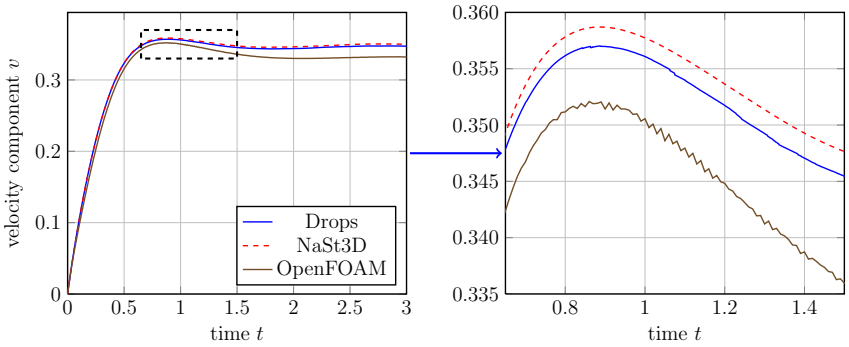

Figure 5: Rise velocity component v for test case 1.

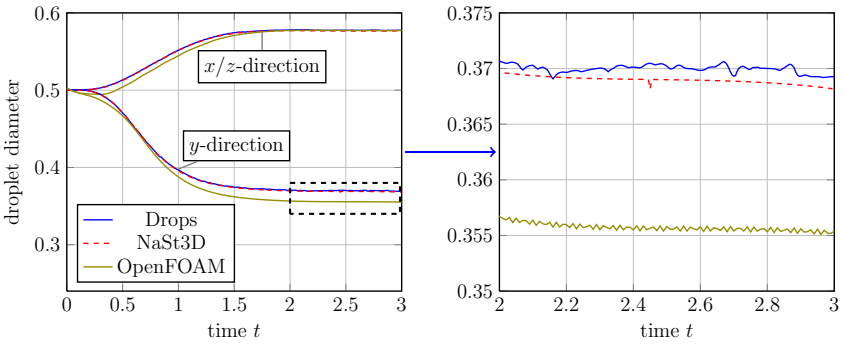

Figure 6: Droplet diameter $\mathbf{d}$ for test case 1.

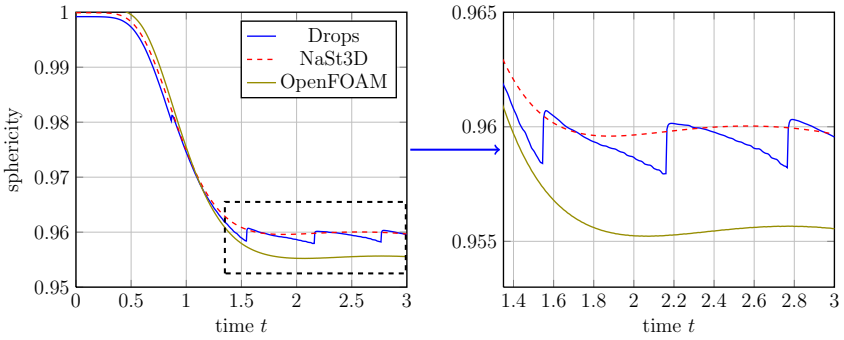

Figure 7: Sphericity Ψ for test case 1.

from the reinitialization of the level set function in DROPS which is performed only when an error threshold of the distance function at the surface is violated. The less frequent reinitialization slightly affects Ψ which is noticeable in Figure 7 but not the other quantities of interest such as $\bar{\mathbf{x}}$ and the rise velocity $\bar{\mathbf{u}}$. All in all, the sphericity results in test case 1 are in high agreement as the differences at steady state are below 0.5% at most.

4.3 Test case 2

Figure 8 shows snapshots of the droplet's temporal evolution in test case 2. In this case, the lower surface tension allows for a stronger droplet deformation as in test case 1. Since test case 2 is located between the skirted and the dimpled ellipsoidal-cap regimes, satellite droplets might occur. All flow solvers do not predict satellite droplets up to a simulated time of $t = 3.5$. However, ongoing simulations show that OpenFOAM predicts 8 satellite droplets at $t \approx 3.9$ that occur pairwise in the direction of each of the lateral four boundary faces.

The differences for the three simulations are most noticeable on the bottom edge of the droplet where the droplet's curvature is largest which is highlighted in Figure 9. Although the droplet shapes in Figure 8 strongly differ at the bottom edge, this is not visible in the two-dimensional contour plot on the plane with normal $\mathbf{n} = (0, 0, 1)^\mathsf{T}$ through the droplet's center as shown on the LHS of Figure 9. The results are identical on an orthogonal plane with normal $\mathbf{n} = (1, 0, 0)^\mathsf{T}$ so that the corresponding contour plot has been omitted. Larger differences can be seen on a further plane with normal $\mathbf{n} = (1, 0, 1)^\mathsf{T}$ that is shown on the RHS of Figure 9. The contour lines on this plane primarily differ at the bottom edge of the droplet at $t \approx 2.5$. As illustrated in a zoomed extract on the RHS of Figure 9, the contour line in NaSt3DGPF (red) on the left/right droplet side is more extended than in DROPS and OpenFOAM. Furthermore, NaSt3DGPF shows a higher contour line at the central part of the bottom side than the other flow solvers. The top edge of all droplets, however, is similar.

The droplet's position over time is visualized in Figure 10. All three flow solvers show a high agreement of the droplet's barycenter position for the whole simulation. Thus, the differences in the contour plot in Figure 9 only slightly affect the droplet's barycenter position. Consequently, $\bar{\mathbf{x}}$ is relatively insensitive with respect to minor variances in the droplet's shape.

The rise velocity plot of the droplet in Figure 11 is also in high agreement for all considered flow solvers. All solvers obtain maximum velocities in the order of 0.37 at $t \approx 0.54$. The droplets' velocity decreases with ongoing time so that a final velocity of $v \approx 0.3$ at $t = 3.5$ is obtained. Here, the results of DROPS and OpenFOAM more resemble each other than the final result of NaSt3DGPF.

In Figure 12, we plot the diameter of the droplet for a better analysis of the droplet's shape. The droplet diameters d_1 and d_3 are in high agreement for all three flow solvers similar to test case 1. There are minor differences in y-direction up to $t \approx 1.6$. The

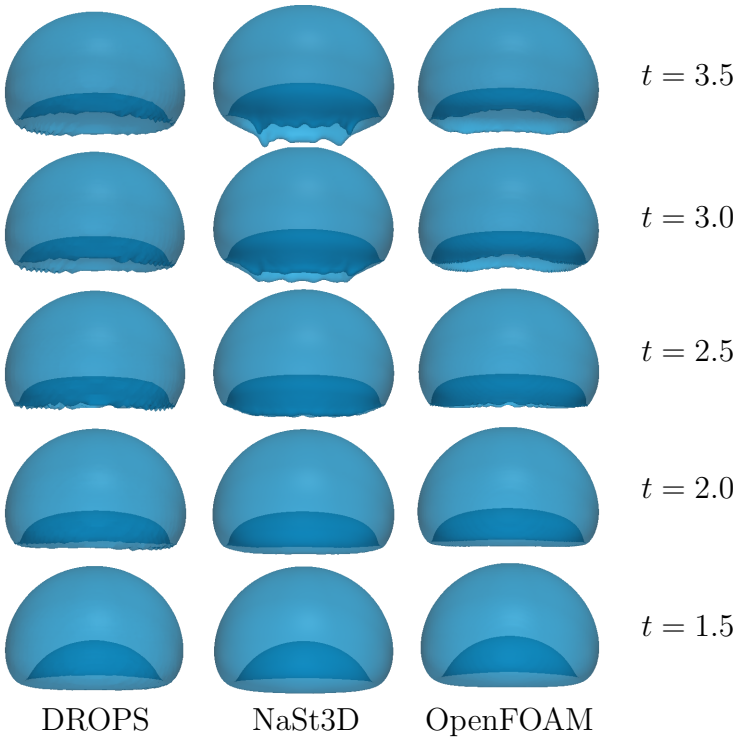

Figure 8: Rising droplet simulation results for test case 2.

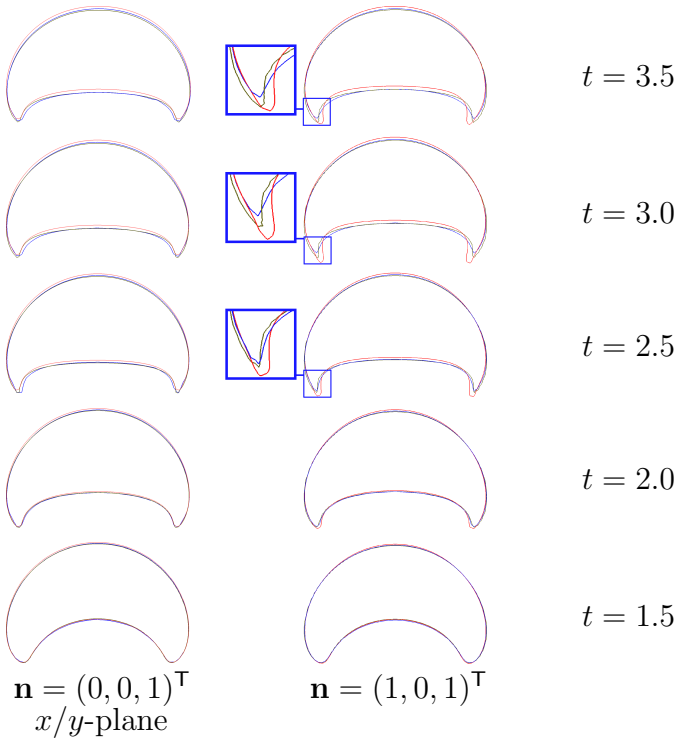

Figure 9: Contour plot of DROPS (blue), NaSt3D (red), OpenFOAM (olive) for test case 2.

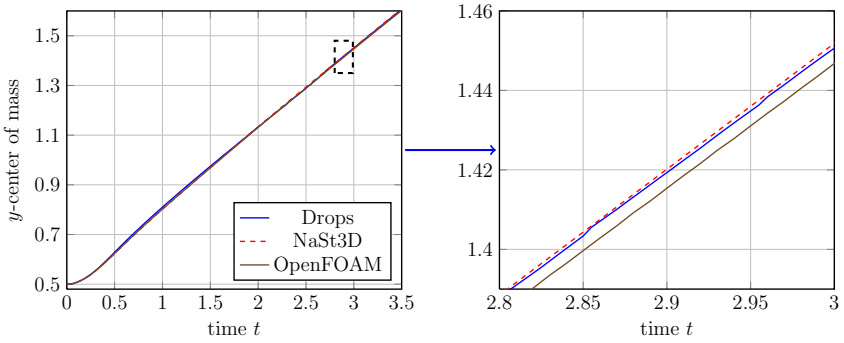

Figure 10: Center of mass $\bar{\mathbf{x}}$ for test case 2.

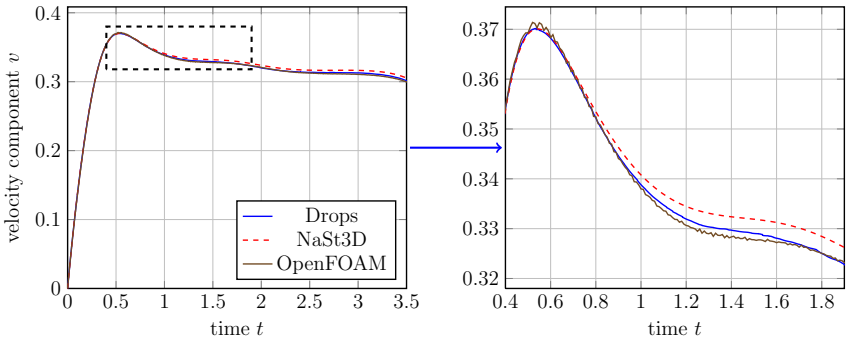

Figure 11: Rise velocity for test case 2.

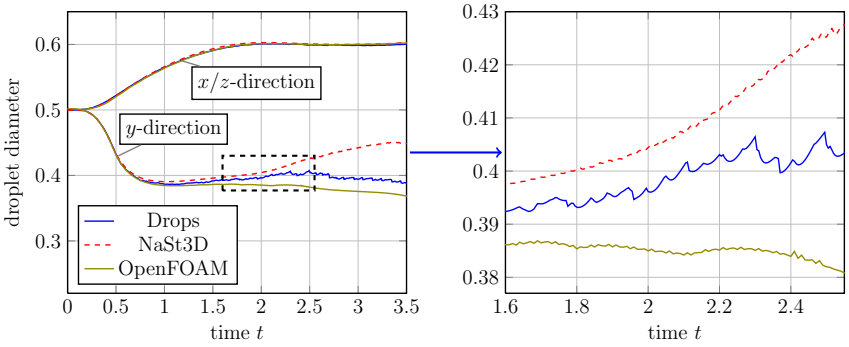

Figure 12: Droplet diameter $\mathbf{d}$ for test case 2.

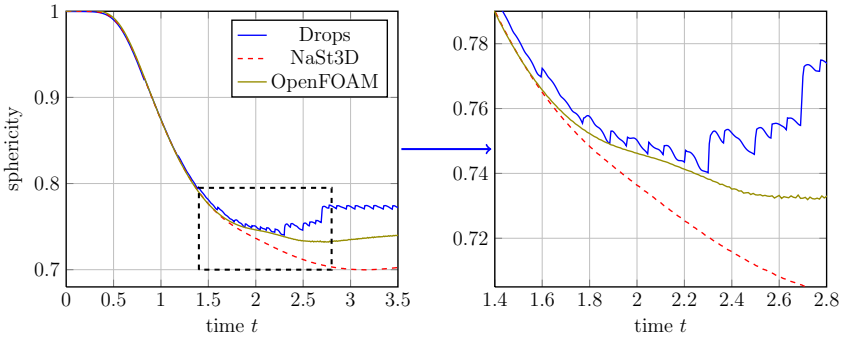

Figure 13: Sphericity Ψ for test case 2.

strong droplet deformation at the left/right edges in NaSt3DGPF then leads to a new rise in the droplet diameter d_2 from its minimum value of about 0.39 up to 0.44 in the final state of the simulation. DROPS and OpenFOAM do not predict a similar new rise in d_2. OpenFOAM shows the largest droplet compression in vertical direction with a minimum value for d_2 of about 0.37.

Finally, Figure 13 shows the sphericity Ψ over time. The results in the early simulation state are similar up to $t \approx 1.6$. DROPS then predicts a more spherical droplet shape which leads to an increase in Ψ at about $t \approx 2.7$. Due to the strong deformation of the droplet in NaSt3DGPF, the flow solver computes an ongoing decrease of Ψ until it reaches a final value of about 0.7. The result for OpenFOAM lies between these two regimes with a final value of about 0.74.

5 CONCLUSIONS

We conducted numerical studies for two different test cases. While the droplet in the first test case experiences only slight deformations, it undergoes strong deformations in test case 2. In general, DROPS and NaSt3DGPF show a high agreement in test case 1 for the defined quantities of interest and for the contour plots. The situation differs for the OpenFOAM results. The general droplet shape is similar to the results of the other flow solvers. This can be seen in the sphericity plot (cf. Figure 7) in which the results differ by 0.5% at most. But, in contrast to DROPS and NaSt3DGPF, OpenFOAM obtains a lower rise velocity in the late state of the simulation so that the droplet's position is shifted in the vertical direction. Although the general shape of the droplet is in high agreement, its position and velocity is controversial. One explanation for these differences might be the different front capturing techniques. DROPS and NaSt3DGPF use the level set technique while OpenFOAM employs the VOF method.

Interestingly, the quantities of interest that were controversial in test case 1 are in relatively high agreement in test case 2 and vice versa. The rise velocity and the droplet's barycenter position resemble each other for the complete simulation period. As the droplet undergoes a strong deformation, it is not surprising that the results for the droplet's diameter and sphericity differ at the end of the simulation. Similar differences occurred in the 2D benchmark experiment by Hysing et al. [1] for test case 2. The actual droplet shape in flow fields with high density and viscosity ratios is a matter of ongoing research. Since the correct droplet shape for the second test case is not even clear in two-dimensional computations, the differences reported in this article are not surprising. In general, the results of DROPS and OpenFOAM show a higher level of agreement than the results of NaSt3DGPF (cf. 3D droplet in Figure 8). These differences might be caused by the usage of different volume correction approaches. While DROPS employs a global volume correction method, NaSt3DGPF uses a local interface preserving algorithm. OpenFOAM makes use of the VOF method so that it is not necessary to enforce an artificial volume correction in this case.

In prospective simulations, we want to perform both simulations on finer meshes to

obtain results that can be used as reference benchmark data for other flow solver. It is also planned to perform simulations using a coupled level set/VOF (CLSVOF) simulation technique. This might deliver further insights into test case 1 in which both front capturing techniques differed in their predictions. Furthermore, it is our aim to encourage other groups to participate in these benchmark simulations so that valid reference data for three-dimensional two-phase flow solvers can be established. For this purpose, we make the data of all quantities of interest available on the website `http://wissrech.ins.uni-bonn.de/research/projects/risingbubblebenchmark`.

ACKNOWLEDGEMENTS

This work was supported by the German Research Foundation DFG via the Hausdorff Center for Mathematics at the University of Bonn in the framework of the German excellence initiative. The authors wish to thank Alisa Geller from the University of Bonn for the analysis and the postprocessing of the benchmark data.

REFERENCES

[1] S. Hysing, S. Turek, D. Kuzmin, N. Parolini, E. Burman, S. Ganesan, L. Tobiska, Quantitative benchmark computations of two-dimensional bubble dynamics, Int. J. Num. Meth. Fluids 60 (11) (2009) 1259–1288.

[2] S. Groß, A. Reusken, Numerical methods for two-phase incompressible flows, Vol. 40 of Springer Series in Computational Mathematics, Springer, 2011.

[3] R. Croce, M. Griebel, M. A. Schweitzer, Numerical simulation of bubble and droplet deformation by a level set approach with surface tension in three dimensions, Int. J. Num. Meth. Fluids 62 (9) (2010) 963–993.

[4] OpenFOAM, The Open Source CFD Toolbox, User Guide Version 2.2.2, `http://www.openfoam.org` (2013).

[5] R. Clift, J. R. Grace, M. E. Weber, Bubbles, drops and particles, Academic Press, New York, London, 1978.

[6] H. Wadell, Volume, shape and roundness of quartz particles, J. Geol. 43 (1935) 250–280.

[7] M. Sussman, E. Fatemi, An efficient, interface preserving level set redistancing algorithm and its application to interfacial incompressible fluid flow, SIAM J. Sci. Comput. 20 (4) (1999) 1165–1191.